An Active Uprighting Mechanism for Flying Robots

Adam Klaptocz, Ludovic Daler, Adrien Briod,
Jean-Christophe Zufferey, and Dario Floreano

***Abstract*—Flying robots have unique advantages in the exploration of cluttered environments such as caves or collapsed buildings. Current systems, however, have difficulty in dealing with the large amount of obstacles inherent to such environments. Collisions with obstacles generally result in crashes from which the platform can no longer recover. This paper presents a method to design active uprighting mechanisms for protected rotorcraft-type flying robots that allow them to become upright and subsequently take off again after an otherwise mission-ending collision. This method is demonstrated on a tailsitter flying robot, which is capable of consistently uprighting after falling on its side using a spring-based "leg" and returning to the air to continue its mission.**

I. Introduction

Flying robots have the unique advantage of being able to provide human operators with an elevated viewpoint of places and objects otherwise inaccessible to people. They are especially useful for exploration of hard-to-reach places such as collapsed buildings, irradiated nuclear power plants, and underground mines that ground-based robots would have trouble navigating because of clutter on the ground. Such environments, however, present flying robots with additional challenges that are not faced in outdoor flight. A lack of reference points, light, or the presence of smoke complicates precise navigation and the presence of many irregular obstacles makes obstacle avoidance very challenging. Even nature's best flying insects occasionally collide with windows or other objects, but are subsequently capable of getting up again and returning to the air through the use of their wings and legs [1], [2].

In this paper, we address the challenge of returning to the air after an uncontrolled landing that may result from a collision. More specifically, we present a method to design active uprighting mechanisms that can be integrated into a protected flying robot, which allows it to stand up and take off again after a fall to the ground. To be successful, it must fulfill three major requirements.

1) *Repeatability:* It must be able to consistently upright the platform from any possible position that it may fall in.
2) *Adaptability to the environment:* It must work on different surface types, angles, and with various amounts of obstacles such as walls or objects.
3) *Integration:* It must not impede the flight capabilities of the robot, and thus remain lightweight, low power, and unobtrusive.

The paper begins by presenting related work in uprighting for robots that move in the air. The following section describes the basic theory involved in uprighting of flying platforms and a method of integrating uprighting into a variety of types of rotorcraft. The method is then applied to design a spring-based uprighting mechanism for a small tailsitter flying robot. An autonomous prototype is then built and a series of tests is performed to evaluate its performance and robustness.

Manuscript received December 1, 2011; revised March 21, 2012; accepted May 14, 2012. Date of publication June 6, 2012; date of current version September 28, 2012. This paper was recommended for publication by Associate Editor T. Hamel and Editor J.-P. Laumond upon evaluation of the reviewers' comments. This work was supported by armasuisse, competence sector Science + Technology for the Swiss Federal Department of Defense, Civil Protection and Sports, and by the Swiss National Science Foundation through the National Centre of Competence in Research Robotics.

The authors are with the Laboratory of Intelligent Systems, Ecole Polytechnique Federale de Lausanne, CH1015 Lausanne, Switzerland (e-mail: adam.klaptocz@epfl.ch; ludovic.daler@epfl.ch; adrien.briod@epfl.ch; jean-christophe.zufferey@epfl.ch; dario.floreano@epfl.ch).

Color versions of one or more of the figures in this paper are available online at http://ieeexplore.ieee.org.

Digital Object Identifier 10.1109/TRO.2012.2201309

II. Related Work

Several flying platforms exhibit the capability of perching (that is controlled landing on a predefined surface) and subsequently taking off again. Most hovering platforms, for example, have landing gear and can land on and take off from flat surfaces, in some cases even autonomously [3]. The morphing micro air and land vehicle [4], a small fixed-wing platform with wheel legs, can land on a flat surface but can only take off again from an elevated position and with a sufficient runway. A glider capable of attaching to a vertical wall and subsequently detach has also been demonstrated [5], as was a powered airplane that can actively return to flight after attachment [6]. All of these systems, however, can only take off if they land in a predefined position and, generally, cannot return to flight from any arbitrary position.

To the best of our knowledge, very few flying platforms have been built specifically with the ability to upright and return to flight. A flying version of the Scout-wheeled robot features an extendable leg meant to upright the platform before flight [7]. This platform, however, is primarily designed as a ground platform and as such has very limited flight capabilities. The first version of the AirBurr robot [8] uses a passive gravity-based technique combined with optimized morphology to return to takeoff position when on the ground. This solution is simple as it does not add any extra actuators to the structure. Its main drawbacks, however, are that it only works on flat ground and that the platform requires substantial free space to return to the air. Any obstacle in its path blocks the takeoff maneuver.

Gravity-based uprighting mechanisms have also been implemented on jumping robots such as the EPFL jumper [9] and the Jollbot [10] and hybrid flying-jumping robots such as the Hopping Rotochute [11] to enable consecutive jumps. All gravity-based mechanisms suffer from the same drawbacks, however, requiring flat and obstacle-free ground to properly upright. Some jumping robots use active mechanisms to upright themselves, such as a series of robots designed by the United States National Aeronautics and Space Administration that use direct actuation of flaps to stand up [12]. The mechanism only works in some landing positions and is not optimized for weight, which is an important consideration for flying systems.

III. Method

In order to devise a method to design an active uprighting mechanism, we must first define the global shape and center of gravity (COG) position of the platform. Cluttered environments require a protective cage around the rotor(s) [8], and thus, most protected rotorcraft can be roughly modeled as truncated cones, with diameter defined by the size of their propellers. Fig. 1 shows the three most common robotic rotorcraft configurations (quadrotors, coaxial helicopters, and tailsitters) and how they fit this general model.

Active uprighting can be reduced to the process of returning a truncated cone to its upright position, ready for vertical takeoff. Due to the symmetry of a cone in the vertical axis, the problem can be further reduced to a 2-D rotation of a mass [as depicted in Fig. 1(D)] about point a through the application of an uprighting force F_u at an arbitrary point d. As the force output of an actuator is, generally, proportional to its weight and power requirements, minimizing this uprighting force is essential for a flying system. Two conditions must be met for this

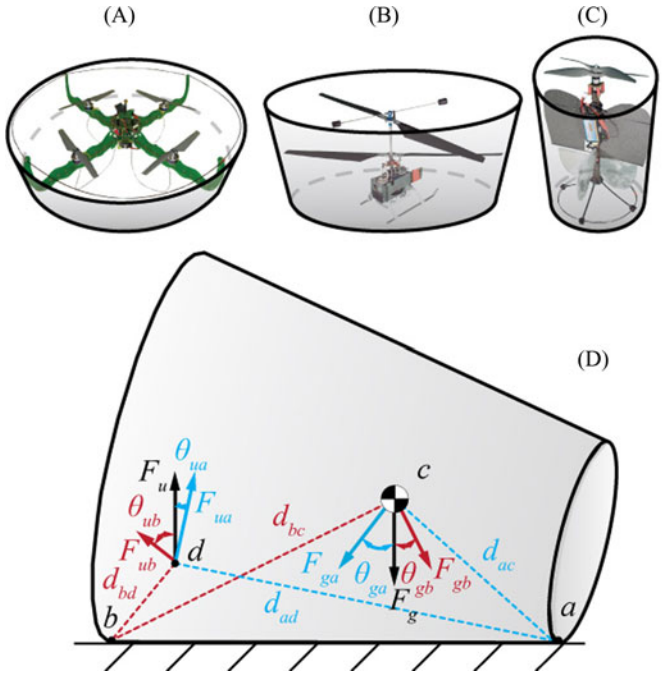

Fig. 1. Three types of hovering platforms that, when adapted with protective cages for flight in cluttered environments, take the general shape of a truncated cone: (A) a quadrotor, (B) a coaxial helicopter, and (C) a tailsitter. (D) Simplified diagram of the same truncated cone on its side before uprighting. A mass with a COG at point c must rotate about point a using uprighting force F_u located at an arbitrary point d to return to the upright position depicted in (A–C).

rotation to occur. First, the uprighting moment created by the force F_u at the point d about point a must be greater than the moment created by gravity acting on the COG with a force F_g. The minimum magnitude of F_u for this condition F_{uamin} follows the equation:

$$F_{\mathrm{uamin}} = \frac{F_g \cos\theta_{ga} d_{ac}}{d_{ad} \cos\theta_{ua}} \tag{1}$$

Second, the uprighting force F_u also creates a moment about point b. There is, thus, also a minimum force F_{ubmin} at which the mass will rotate around point b, which follows a similar equation. As neither points a nor b are fixed to the surface, in order for the mass to rotate around point a and not point b, F_{uamin} must be less than F_{ubmin}:

$$F_{\mathrm{uamin}} < F_{\mathrm{ubmin}} \tag{2}$$

$$\frac{\cos\theta_{ga} d_{ac}}{d_{ad} \cos\theta_{ua}} < \frac{\cos\theta_{gb} d_{bc}}{d_{bd} \cos\theta_{ub}}. \tag{3}$$

Equations (1) and (3) provide interesting insight into the position, direction, and magnitude of the uprighting force F_u and the position of the COG required for rotation around point a. It can be summarized as follows.

1) The COG c should be as close to the rotation point a as possible, as minimizing d_{ac} decreases F_{gamin} (1). In addition, moving the COG to the right toward point a moves it away from point b, increasing d_{bc}, and thus increasing F_{ubmin}.
2) If the COG can be moved to the right of point a, the angle θ_{ga} and, subsequently, F_{gamin} become negative (1). This corresponds to the case of *gravity-based uprighting* [8] where no uprighting force is required.
3) Point d should be as far as possible from point a and as close as possible to point b to avoid rotation around point b (3).

Implementing the previous guidelines in the design of an active uprighting mechanism is not always a straightforward process as aerodynamics, weight, morphology, position of control surfaces, and the COG must all be balanced in order for the platform to be able to fly. Simple changes to the platform's morphology, however, such as modifying the protective cage (and thus contact points a and b) can facilitate uprighting without significantly affecting flight performance.

Once a platform type is selected and its morphology adapted for active uprighting, the next step is to select a method to generate the uprighting force F_u. Using existing rotors (in forward or reverse) has the great advantage of not adding any weight to the platform and should be used whenever possible. The force available from onboard rotors, however, is limited due to several reasons; the force is not always in the desired direction throughout uprighting, rotors turning in reverse are less efficient and the individual rotors of a multirotor system provide limited force. To increase uprighting efficiency, thrust can be vectored in the desired direction using smartly placed control surfaces or by rotating the motors, although at the cost of additional mechanical components, servo-motors, and increased complexity.

When on-board rotors do not suffice, an additional mechanism must be implemented. One example consists of a beam attached to the platform that pushes against the ground and is powered by an additional actuator such as a DC motor.

As the platform rotates around point a, the direction of the uprighting force may change, as does the force due to the weight of the platform. A model should, thus, be created based on (1) and (3) to evaluate the required force during the entire uprighting action to dimension the force generation method to provide enough uprighting force.

To summarize, these are the steps in our method to design active uprighting systems.

1) Choose a platform type (quadrotor, coaxial, etc.).
2) Modify cage morphology to facilitate uprighting.
3) Choose uprighting force generation method(s).
4) Model method throughout uprighting action.
5) Build and integrate into flying system.

IV. Demonstration on a Tailsitter Robot

In this paper, we use the AirBurr platform as a proof of concept to demonstrate the presented method. The AirBurr robot is a coaxial tailsitter design that was first introduced in [8]. The core of the robot is based on a central vertical fuselage topped with two main motors for lift and yaw control. The center of the fuselage contains the control electronics and the battery. The bottom of the fuselage contains the control surfaces used for roll and pitch control.

To make the platform robust to contact, it is surrounded with a protective cage made of carbon fiber. The cage is designed to be larger near the propellers and smaller near the control surfaces to facilitate uprighting according to the guidelines in Section III. In addition, the top of the cage is extended and ends in a point, facilitating gravity-based uprighting (see [8]).

When the robot lands on its top, the placement of the COG and the shape of the cage will make it rotate onto its side using gravity alone (see [8]). When it lands on its side, however, the main rotors cannot provide force in the correct direction to upright the platform, as they are almost inline with the bottom ring (rotation point a) and, thus, provide little uprighting torque. An additional mechanism using extending "legs" attached to the fuselage through a spring is, thus, chosen.

A model based on (1) and (3) is used to evaluate the force required from the legs at various attachment points [see Fig. 3(A)] to optimize the size of the spring and the attachment point of the legs during the entire

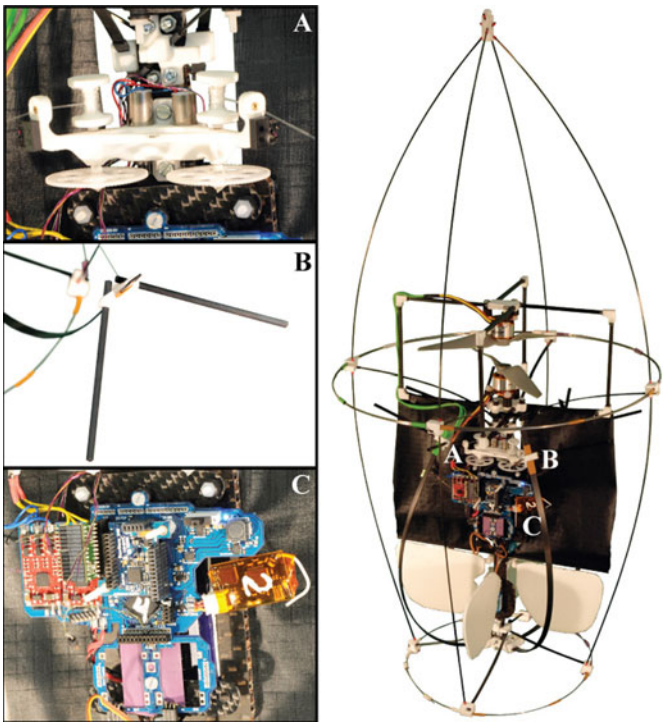

Fig. 2. AirBurr prototype with integrated active uprighting mechanism. (A) shows one half of the rollup mechanism used to close the legs for flight. (B) shows the end of the "leg" with attached "feet" for stability. (C) shows the control electronics and on-board sensors.

uprighting process [see Fig. 3(B)]. Fig. 3(C) shows the varying spring factor profiles based on the spring's attachment point to the fuselage. As the attachment point moves from the bottom of the platform to the top, the initial spring factor decreases since the length of the leg decreases. However, the angle between the leg and the ground increases, and thus, a smaller component of the force at the tip of the leg is used to upright the platform. There is, thus, an optimal attachment position of 80 mm [see Fig. 3(D)] from the back of the platform at which the spring constant k, and thus the size of the spring, is minimized. It should be noted, however, that any attachment point of less than 110 mm from the bottom ring will provide a spring factor within 15% of the minimum possible value.

The modified cage and leg mechanism are then integrated into the AirBurr platform, as seen in Fig. 2. The platform requires four legs, one for each quadrant, to be able to upright from any possible position on its side. Instead of using a stiff (and thus heavy) leg attached to a high-torque (also heavy) spring, we use flexible carbon-fiber beams that integrate the spring within the leg itself. The legs are dimensioned to provide the spring factor required by the model and are anchored near the optimal attachment point using 3-D-printed plastic. Two carbon-tube "feet" at the end of each beam [see Fig. 2(B)] provide a more stable anchor point on uneven ground. The legs are retracted using nylon string attached to their tips, which are rolled up using four individual DC motors with a 225:1 gear ratio [see Fig. 2(A)]. Retraction is detected using infrared (IR) proximity sensors.

The AirBurr robot is controlled by a motherboard, called the BurrMove, and a system of daughter boards, all designed in-house [see Fig. 2(C)]. The BurrMove printed circuit board includes power management, actuation for flight motors, control surfaces and DC motors, and a radio receiver. The daughter boards contain accelerometers and gyroscopes required by the inertial measurement unit (IMU), a radio connection to a base station and four IR sensors.

A simple autonomous uprighting controller is implemented on top of the regular flight controller. The controller uses the accelerometer (also used for flight control) to detect the orientation of the platform. If the controller detects that the platform is on its side, it will unravel all four legs to return the platform to a vertical position. Once the platform is vertical and standing on its bottom ring, all legs are retracted into their closed position, ready for takeoff.

V. Results

A working prototype of the platform is put through a series of tests to evaluate its performance based on the design requirements: repeatability, adaptability to the environment, and integration. A successful uprighting is one that can return the platform to an upright position ready for takeoff, that is, with an angle between the ground and the fuselage of more than 70°.

A. Repeatability

The first round of tests is aimed at measuring repeatability of the uprighting motion on flat, smooth ground to show that the uprighting motion is independent of the starting position. The platform is placed upright, manually knocked over 20 times in random directions and subsequently uprighted using the autonomous controller. Fig. 4(A) shows the angle along the axis of the fuselage facing the ground during uprighting, calculated using the on-board IMU. As the legs extend, the platform rotates until two of the four legs are touching the ground, which occurs in the first 5–10 s of the uprighting maneuver. These two legs and the back ring form three points of contact and, thus, a stable orientation for the rest of the uprighting maneuver. As there are four legs symmetrically spaced around the platform, there are four stable positions during uprighting, as can be seen in the figure. A typical uprighting sequence is shown in Fig. 5.

Fig. 4(B) plots the angle between the fuselage and the ground (uprighting angle) for each uprighting trial. Irrespective of the starting position, the platform consistently uprights at the same speed, between 20 and 25 s. The speed is limited by the motor and gear ratio selected for the rollup mechanism, which are optimized for weight rather than speed. This test successfully demonstrates the ability of the robot to consistently upright irrespective of its starting ground position.

B. Adaptability to the Environment

The next set of experiments tests the mechanism's adaptability to differences in surrounding obstacles, ground angles, and surface textures. In each case, the experiment is run five times using the autonomous controller and five times, using individual manual control of the four legs, by a human operator. The success rate of the various experiments is shown in Fig. 6.

The first set of experiments varies the angle of the ground between $-15°$ and $+15°$ to simulate the often uneven ground found in unstructured environments. A second set of experiments varies the ground texture between hardwood, carpet (found in typical indoor office environments), gravel (found in outdoor environments), and small rocks (to simulate a cave environment). A third experiment evaluates the performance of the mechanism in right-angle corners, a common and difficult landing position for flying robots after a collision. The prototype is placed on its side in a right-angle corner on hardwood, with its base pointing first toward and then away from the corner.

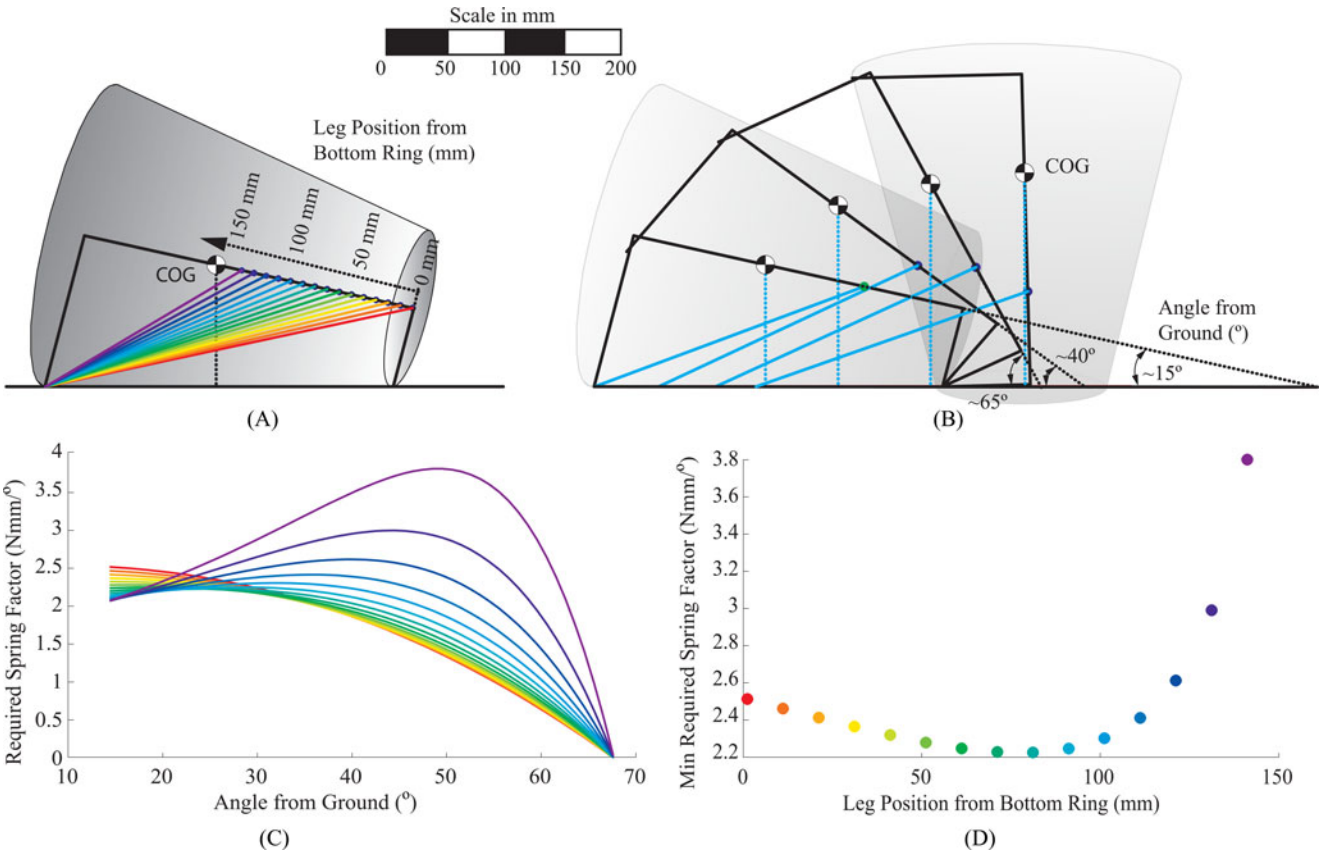

Fig. 3. Optimization of leg attachment position on the fuselage. (A) shows the different attachment positions modeled, each with a respective color. The leg is made as long as possible while still remaining within the protective cage when retracted. All of these attachment positions will result in a rotation around the bottom ring and not the top ring (3). (B) shows four example positions during the uprighting process. (C) plots the required spring factor at each angle during uprighting. (D) plots the minimum spring factor that must be dimensioned for uprighting to be successful.

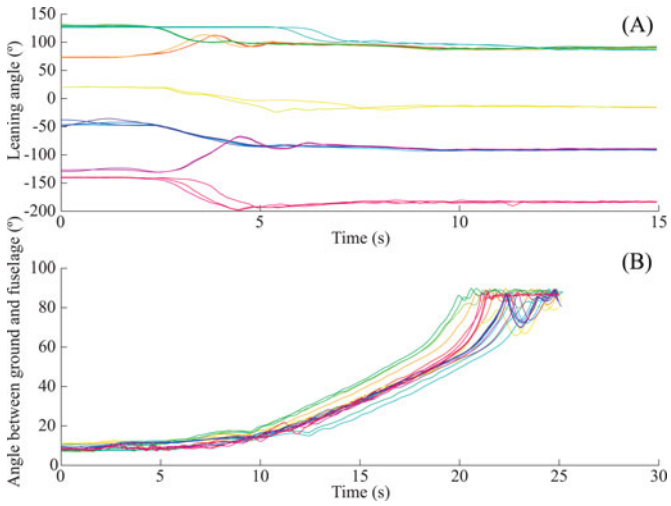

Fig. 4. Platform orientation sequences during 20 uprighting maneuvers, each denoted by a different shade. (A) plots the robot's leaning angle. (B) plots the angle between the fuselage and the ground during uprighting.

As demonstrated, the mechanism works successfully in many common situations. In the cases where uprighting does not succeed, there are several ways of increasing the success rate.

1) When the ground angle is below $-15°$[see Fig. 6(A)], the force from the legs is only able to partially upright the platform. In most of these cases, the platform is vertical enough to still be able to take off, stabilize, and close its legs.
2) When the ground angle is above $+15°$, the platform topples over itself and falls down the slope. In these cases, once again the platform can take off before being fully upright, or close its legs and upright a second time.
3) High-surface roughness can cause the carbon "feet" to occasionally get stuck [see Fig. 6(B)]. Retracting and then reextending the legs can help the feet get unstuck.
4) Extending all four legs at once is not well suited for difficult situations, such as corners [see Fig. 6(C)], where the legs simultaneously push against walls or other obstacles. In such situations, simply extending some legs and not others will lead to successful uprighting.

Most of the failure modes are due to the simplicity of the on-board automatic controller, which only opens or closes the four legs all at once.

C. Integration Into Flight Systems

The final experiment demonstrates that the mechanism can be integrated into a flying robot and not impede on its primary activity of flying. The total weight of the mechanism, including legs, rollup mechanism, sensors, and electronics is 39.8 g, which represents 16% of the

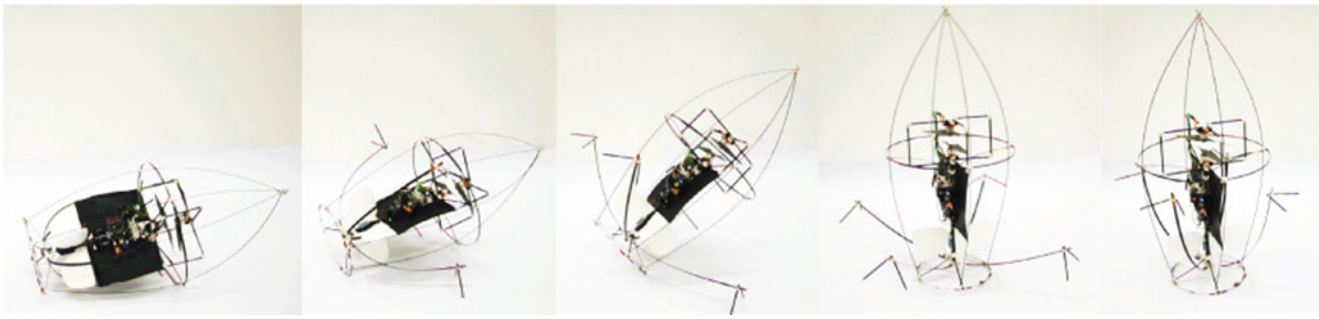

Fig. 5. From left to right, a typical uprighting sequence using the autonomous controller.

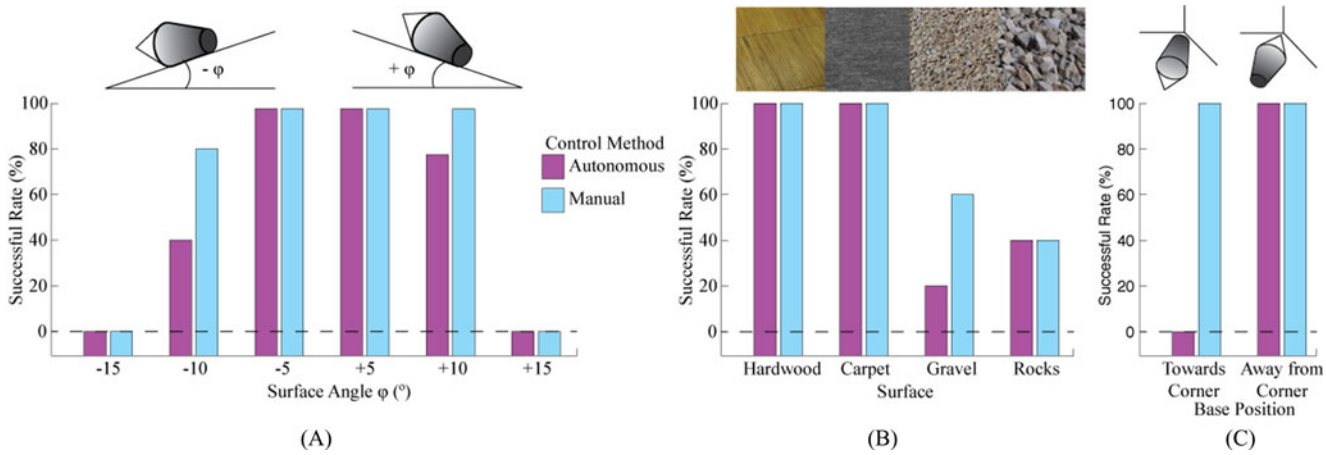

Fig. 6. Uprighting success rate for various environments based on five trials using the autonomous controller (purple) and five trials by a human operator (blue). (A) plots uprighting on ground angles between +/−15°. (B) plots uprighting in various surface textures. (C) plots uprighting in corners.

total weight of the platform (250 g). The symmetry of the mechanism about the fuselage does not significantly alter the COG or the flight aerodynamics of the entire platform. The extra weight does, however, reduce flight time from an average of 4:21 to 2:11 min (based on three flights in each configuration with a full battery).

A series of five test flights are performed during which the robot is kept flying for approximately 30 s, then purposely flown into a wall causing the platform to drop to the flat, obstacle-free ground. In all cases, the robot is able to upright itself autonomously and return to flight within 30 s of the collision. A sample of these flights can be seen in the accompanying video.

VI. Conclusion

In this paper, we introduced the basic theory of uprighting of a rotorcraft platform after a collision as well as a method to design active uprighting mechanisms that can be applied to many types of flying robots. We, then, implemented the method on a tailsitter robot that is capable of consistently uprighting the platform, preparing it for subsequent takeoff. The mechanism was successful in a variety of environmental conditions, including uneven terrain, varying surface textures, and tight corners. Such a mechanism is a key requirement in enabling flying robots to explore confined, cluttered environments where contact with obstacles is inevitable.

The active uprighting mechanism described in this paper is a first mechanical implementation that could be extended through improved sensing and control. Initial investigations show that lightweight strain gauges integrated into the legs can measure the shape of the leg and, thus, the force it provides at its tip. Further, strain gauges can measure tension in the string and, thus, contact with obstacles. Such information can be leveraged to create a more intelligent controller that can extract the platform from ever more complex situations.

References

[1] A. A. Faisal and T. Matheson, "Coordinated righting behaviour in locusts," *J. Exp. Biol.*, vol. 204, no. 4, pp. 637–648, 2001.

[2] L. Frantsevich, "Righting kinematics in beetles (Insecta: Coleoptera)," *Arthropod Struct. Develop.*, vol. 33, pp. 221–235, 2004.

[3] D. Cabecinhas, R. Naldi, L. Marconi, C. Silvestre, and R. Cunha, "Robust take-off and landing for a quadrotor vehicle," in *Proc. IEEE Int. Conf. Robot. Autom.*, May 2010, pp. 1630–1635.

[4] F. Boria, R. Bachmann, P. Ifju, R. Quinn, R. Vaidyanathan, C. Perry, and J. Wagener, "A sensor platform capable of aerial and terrestrial locomotion," in *Proc. IEEE/RSJ Int. Conf. Intell. Robots Syst.*, 2005, pp. 4024–4029.

[5] M. Kovač, J. Germann, C. Hürzeler, R. Y. Siegwart, and D. Floreano, "A perching mechanism for micro aerial vehicles," *J. Micro-Nano Mechatronics*, vol. 5, pp. 77–91, 2010.

[6] A. Desbiens, A. Asbeck, and M. Cutkosky, "Scansorial landing and perching," in *Robotics Research*. New York: Springer, 2011, pp. 169–184.

[7] A. Kossett and N. Papanikolopoulos, "A robust miniature robot design for land/air hybrid locomotion," in *Proc. IEEE Int. Conf. Robot. Autom.*, 2011, pp. 4595–4600.

[8] A. Klaptocz, G. Boutinard-Rouelle, A. Briod, J.-C. Zufferey, and D. Floreano, "An indoor flying platform with collision robustness and self-recovery," in *Proc. IEEE Int. Conf. Robot. Autom.*, 2010, pp. 3349–3354.

[9] M. Kovač, M. Schlegel, J.-C. Zufferey, and D. Floreano, "Steerable miniature jumping robot," *Autonomous Robots*, vol. 28, pp. 295–306, 2010.

[10] R. Armour, "A biologically inspired jumping and rolling robot," Ph.D. dissertation, Univ. Bath, Bath, U.K., 2010, 2012.
[11] E. Beyer and M. Costello, "Performance of a hopping rotochute," *Int. J. Micro Air Veh.*, vol. 1, pp. 121–137, 2009.
[12] P. Fiorini and J. Burdick, "The development of hopping capabilities for small robots," *Autonomous Robots*, vol. 14, pp. 239–254, 2003.

Three-DOF Microrobotic Platform Based on Capillary Actuation

Cyrille Lenders, Michaël Gauthier, Rémi Cojan, and Pierre Lambert

***Abstract*—This paper presents a new microrobotic platform actuated by capillary effects, combining surface tension and pressure effects. The device has 6 degrees of freedom (DOFs), among which, three are actuated: the z-axis translation having a stroke of a few hundreds of microns and θ_x and θ_y tilting up to about 15°. The platform is submerged in a liquid and placed on microbubbles whose shapes (e.g., height) are driven by fluidic parameters (pressure and volume). The modeling of this new type of compliant robot is described and compared with experimental measurements. This paper paves the way for an interesting actuation and robotic solution for submerged devices on the microscale.**

***Index Terms*—Fluidic actuators, manipulation and compliant assembly, micro/nanorobots, surface tension.**

I. Introduction

Microassembly deals with the assembly of submillimetric components. The operations that consist of gripping, moving, placing, and releasing microcomponents to defined locations have to deal with forces inherent to the microworld. To minimize the effects of some of these forces, which are difficult to control, a strategy consists in performing the manipulation in a liquid [10].

To achieve the objective of automated assembly of microcomponents, there is a growing need for new devices addressing the current problems of microassembly. These include the structure's lack of compliance, which, combined with positioning and manufacturing errors, can lead to the destruction of the components [4], [20].

Some authors have proposed to include compliance in the grippers [6], [12], [21], [23], but the drawback of such devices is the risk of oscillation when accelerating the gripper. Other authors have proposed to include compliance in the support table, based on the use of springs [4]. However, these systems are generally bulky or fragile if a low stiffness is required. Besides, these systems cannot be easily actuated. We propose in this paper a novel compliant table to perform assembly operations, which is based on the use of surface tension effect of gaseous bridges (bubbles) between two solids in a liquid. Such a table could be used as a support for assembly operations, with a moving microgripper bringing new components and assembling them. For reference, the vertical stiffness of the device proposed in [4] is 6.7 Nm^{-1}, which is of the same order of magnitude as for our system.

Using bubbles as a means of actuation for microsystems has already been investigated, but these investigations are generally based on the expansion or coalescence of bubbles [19]. Moreover, the compliance is not taken into account [9].

The objective of this paper is to present the microbubble-based actuation system, a model to predict its stiffness behavior and, finally, to show the advantages of such a system.

Manuscript received October 14, 2011; revised March 18, 2012; accepted May 4, 2012. Date of publication July 3, 2012; date of current version September 28, 2012. This paper was recommended for publication by Associate Editor Y. Sun and Editor B. J. Nelson upon evaluation of the reviewers' comments. This work was supported by the Bureau des Relations Internationales et de la Coopération from the Université libre de Bruxelles and PHC-Tournesol (WBI-FNRS EGIDE).

C. Lenders and P. Lambert are with the Department of Bio-, Electro-, and Mechanical Systems, Université libre de Bruxelles, 1050 Bruxelles, Belgium (e-mail: clenders@ulb.ac.be; plambert@ulb.ac.be).

M. Gauthier and R. Cojan are with the Department of Automatic Control and Micro-Mechatronic Systems, FEMTO-ST Institute, UMR CNRS 6174-UFC ENSMM UTBM, 25000 Besançon, France (e-mail: michael.gauthier@femto-st.fr; remi.cojan@gmail.com).

Color versions of one or more of the figures in this paper are available online at http://ieeexplore.ieee.org.

Digital Object Identifier 10.1109/TRO.2012.2199009

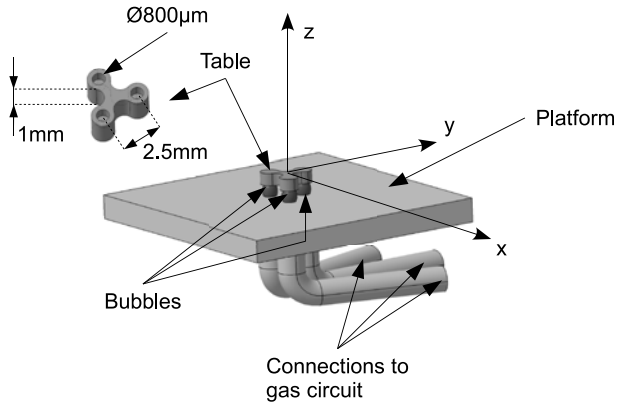

Fig. 1. Schematic view of the device, composed of a compliant table lying on three bubbles generated from a platform.

II. Device Overview

The device presented here is a compliant platform that can be used to perform microrobotic assembly tasks in a liquid environment. The table has 6 degrees of freedom (DOFs), among which, three are actuated: the translation along the direction orthogonal to the platform plane $\vec{z}$ and two rotations along axes parallel to the platform plane.

The device is made out of three main components [14]: the moving table, the three bubbles which are used as compliant actuators, and the platform from which the bubbles are generated (see Fig. 1).

Bubbles are the key to this device. Thanks to surface tension at the gas–liquid interface, and to the gas compressibility, a microbubble can be used as a compliant actuator. Indeed, the force developed by a bubble sandwiched between two solids has two components: one due to surface tension along the triple line (where solid, liquid, and gas touch one another), and the other due to the pressure gradient across the interface. If the contact angles in the liquid are smaller than 90°, the mean curvature of the bubble interface is positive, and the pressure inside the bubble is larger than in the surrounding liquid. When the bubble is squeezed, it is compressed and exerts a repulsive force on the solids. When it is stretched, it exerts an attractive force on the solids. Its behavior is comparable to a spring, from a mechanical point of view. However, we will demonstrate that using a bubble presents several advantages compared with classical mechanical springs. One of these advantages is that it is possible to actuate bubbles using the fluidic parameters pressure P and volume V.

To control the actuator, it is necessary to control the bubbles generation. We propose to use a system derived from a syringe pump: The idea